

MASS ACCRETION RATE OF ROTATING VISCOUS ACCRETION FLOW

MYEONG-GU PARK^{1,2}

¹ Department of Astronomy and Atmospheric Sciences, Kyungpook National University, Daegu, Republic of Korea; mgp@knu.ac.kr

² Department of Astrophysical Sciences, Princeton University, Princeton, NJ, USA

Received 2008 July 28; accepted 2009 October 9; published 2009 November 3

ABSTRACT

The mass accretion rate of transonic spherical accretion flow onto compact objects such as black holes is known as the Bondi accretion rate, which is determined only by the density and the temperature of gas at the outer boundary. A rotating accretion flow has angular momentum, which modifies the flow profile from the spherical Bondi flow, and hence its mass accretion rate, but most work on disc accretion has taken the mass flux to be given with the relation between that parameter and external conditions left uncertain. Within the framework of a slim α disk, we have constructed global solutions of the rotating, viscous, hot accretion flow in the Paczyński–Wiita potential and determined its mass accretion rate as a function of density, temperature, and angular momentum of gas at the outer boundary. We find that the low angular momentum flow resembles the spherical Bondi flow and its mass accretion rate approaches the Bondi accretion rate for the same density and temperature at the outer boundary. The high angular momentum flow on the other hand is the conventional hot accretion disk with advection, but its mass accretion rate can be significantly smaller than the Bondi accretion rate with the same boundary conditions. We also find that solutions exist only within a limited range of dimensionless mass accretion rate $\dot{m} \equiv \dot{M}/\dot{M}_B$, where \dot{M} is the mass accretion rate and \dot{M}_B is the Bondi accretion rate: when the temperature at the outer boundary is equal to the virial temperature, solutions exist only for $0.05 \lesssim \dot{m} \leq 1$ when $\alpha = 0.01$. We also find that the dimensionless mass accretion rate is roughly independent of the radius of the outer boundary but inversely proportional to the angular momentum at the outer boundary and proportional to the viscosity parameter, $\dot{m} \simeq 9.0 \alpha \lambda^{-1}$ when $0.1 \lesssim \dot{m} \lesssim 1$, where the dimensionless angular momentum measure $\lambda \equiv l_{\text{out}}/l_B$ is the specific angular momentum of gas at the outer boundary l_{out} in units of $l_B \equiv GM/c_{s,\text{out}}$, M is the mass of the central black hole, and $c_{s,\text{out}}$ is the isothermal sound speed at the outer boundary.

Key words: accretion, accretion disks – black hole physics – quasars: general – X-rays: general

1. INTRODUCTION

The amount of mass gravitationally accreted to the compact objects such as black holes is determined by the conditions of gas around the compact objects. The case when gas has a spherically symmetric distribution, a polytropic pressure–density relation, and no angular momentum was solved by Bondi (1952), who found that the mass accretion rate for the transonic accretion is determined only by the density and the temperature of surrounding gas, both assumed to approach constant values far from the accreting objects. This rate, known as the Bondi accretion rate, is widely used as “the mass accretion rate” in a variety of accretion problems. As a function of the density ρ_∞ and the isothermal sound speed $c_{s,\infty}$ of gas at infinity, the Bondi rate for pure hydrogen gas is

$$\dot{M}_B = 4\pi\Lambda \frac{(GM)^2 \rho_\infty}{\gamma^{3/2} c_{s,\infty}^3}, \quad (1)$$

where G is the gravitational constant, M is the mass of the central object, and γ is the adiabatic index of accreting gas. The constant $\Lambda(\gamma)$ is 0.25 for $\gamma = 5/3$ and 1.12 for $\gamma = 1$. If we define the Bondi radius as $r_B \equiv GM/c_{s,\infty}^2$, then $\dot{M}_B = \Lambda\gamma^{-3/2} 4\pi r_B^2 \rho_\infty c_{s,\infty}$. Gravity starts to dominate over gas pressure inside the Bondi radius, and the Bondi accretion rate is roughly the mass flux of gas infalling into a sphere of radius r_B with a velocity equal to the sound speed at infinity.

However, many astrophysical accretion flows are expected to have certain amount of angular momentum, and the angular momentum will surely affect the flow properties, including the mass accretion rate. Surprisingly, the rate of mass accretion for

these rotating, viscous accretion flows for given external boundary conditions has not been studied yet. We might expect that if the rotational support is negligible at the Bondi radius, the effect of angular momentum to mass accretion rate would be small. But the accretion rate would diminish as the dimensionless measure of rotation $\lambda \equiv l_{\text{out}}/l_B$ approaches unity, where l_{out} is the specific angular momentum of gas at the outer boundary and $l_B \equiv r_B c_{s,\infty}$ is the representative angular momentum expected at the Bondi radius.

Although the accretion problem can be reduced to local one in the limit of thin accretion disk where the radial velocity is negligible (Shakura & Sunyaev 1973), accretion flow is fundamentally global in the sense that the flow structure is only globally determined. As pointed out by Yuan (1999), the flow property can be qualitatively affected by the outer boundary conditions. The dependence of the mass accretion rate on boundary conditions can only be addressed by constructing global solutions. There have been many studies on the global solutions of rotating accretion flow (e.g., Narayan et al. 1997; Chen et al. 1997; Nakamura et al. 1997; Lu et al. 1999) and the effects of outer boundary conditions on accretion flow (Yuan 1999; Yuan et al. 2000), but most have focused on the flow structures and emission properties for a given mass accretion rate, and the determination of how that rate is fixed by external circumstances remains to be addressed.

In this work, we focus on the mass accretion rate of the accretion flow, especially its dependence on the density, temperature, and the angular momentum of gas at the outer boundary. We do this by constructing the simplest global, transonic solutions within the slim disk formalism (Abramowicz et al. 1988). The slim disk formalism uses vertical integration to take into account

the finite thickness of the accretion disk, and more importantly allows for the radial motion of the accretion flow and the critical point unlike the thin disk approximation (Shakura & Sunyaev 1973).

2. EQUATIONS AND METHODS

2.1. Equations

In the slim disk approximation, the continuity equation is

$$\dot{M} = -4\pi r H \rho v_r, \quad (2)$$

where v_r is the radial velocity ($v_r < 0$ for inflow) and ρ is the density of the flow, both averaged over the height of the disk. The disk scale height is $H \equiv c_s/\Omega_K$, where the isothermal sound speed $c_s^2 \equiv P/\rho$, P is the total gas pressure, and Ω_K is the Keplerian angular velocity for the Paczyński–Wiita potential (Paczyński & Wiita 1980). This treatment allows for the general relativistic effect in an approximate fashion.

We assume that the gas is composed of hydrogen only and is fully ionized. Ions and electrons are assumed to have the same temperature T , and hence in this simplified treatment of a pure hydrogen gas, the gas pressure is $P = (n_p + n_e)kT = 2n_p kT = 2(\rho/m_p)kT$, where n_p and n_e are the number densities of protons and electrons, respectively, m_p is the proton mass, and k is the Boltzmann constant.

The radial momentum equation is

$$v_r \frac{dv_r}{dr} + (\Omega_K^2 - \Omega^2)r + \frac{1}{\rho} \frac{dP}{dr} = 0, \quad (3)$$

where $\Omega(r)$ is the angular velocity at radius r . Since we adopt the Paczyński–Wiita potential, the Keplerian angular velocity is $\Omega_K^2(r) \equiv GMr^{-3}[1 - (r_{\text{Sch}}/r)]^{-2}$, where $r_{\text{Sch}} \equiv 2GM/c^2$ is the Schwarzschild radius and c is the speed of light.

The angular momentum equation is given by

$$\rho v_r (\Omega r^2 - l_0) = \eta \alpha P, \quad (4)$$

where the constant α is the viscosity parameter of Shakura & Sunyaev (1973): the viscous stress tensor $\tau_{\phi r} = -\alpha P$ (Abramowicz et al. 1988). Depending on exactly how the viscosity description is implemented, the parameter η can be from $\eta = -2$ (Abramowicz et al. 1988), $\eta = -1$ (Nakamura et al. 1997), $\eta = (r/\Omega_K)(d\Omega/dr)$ (Narayan et al. 1997) to $\eta = d \ln \Omega_K / d \ln r$ (Narayan et al. 1997; Yuan 1999). We choose $\eta = -1$ because this choice simplifies the angular momentum equation into an algebraic one and has an added convenience of automatically satisfying the no-torque condition at the black hole horizon (Abramowicz et al. 1988; Yuan et al. 2000). On the other hand, this implementation overestimates the shear stress when there is little or no shear, and can cause difficulties when the solution is extended to a very large radius. The integration constant l_0 is the specific angular momentum accreted by the black hole, to be determined as the eigenvalue during the construction of solutions for given boundary conditions.

Finally, the energy equation is

$$\rho v_r \left[\frac{d\epsilon}{dr} + P \frac{d}{dr} \left(\frac{1}{\rho} \right) \right] = q^+ - q^-, \quad (5)$$

where $\epsilon = (\gamma - 1)^{-1} P/\rho$ is the internal energy of the gas per unit mass, q^+ and q^- are the heating and cooling functions per

unit volume, respectively. The only heating process considered in the current treatment is the viscous heating, for which we use the description

$$q_{\text{vis}}^+ = -\zeta \alpha P r (d\Omega/dr). \quad (6)$$

We fix $\zeta = 1$ as in Abramowicz et al. (1988), Nakamura et al. (1997), and Yuan et al. (2000). Slightly different values of ζ have been used in other works: for example, $\zeta = -(r/\Omega_K)(d\Omega/dr)$ by Narayan et al. (1997) and $\zeta = -(d \ln \Omega_K / d \ln r)$ by Yuan (1999).

Since we mainly deal with a high-temperature accretion disk with significant radial velocity, we use the optically thin, relativistic ion–electron bremsstrahlung as the only cooling process:

$$q^- = \alpha_f r_e^2 m_e c^3 n_p n_e (32/3)(2/\pi)^{1/2} \left(\frac{kT}{m_e c^2} \right)^{1/2} \times \left[1 + 1.78 \left(\frac{kT}{m_e c^2} \right)^{1.34} \right], \quad (7)$$

where α_f is the fine structure constant, r_e is the classical electron radius, and m_e is the electron mass (Svensson 1982 and references therein).

Equations (3) and (5) can be rearranged into the form

$$\frac{dv_r}{dr} = \frac{A}{D}; \quad \frac{dc_s}{dr} = \frac{B}{D}, \quad (8)$$

where

$$A \equiv - \left(\frac{\gamma + 1}{\gamma - 1} + 2\zeta \eta \alpha^2 \frac{c_s^2}{v_r^2} \right) v_r \left[(\Omega_K^2 - \Omega^2)r + \frac{rc_s^2}{\Omega_K} \frac{d}{dr} \left(\frac{\Omega_K}{r} \right) \right] - v_c^2 \frac{r}{\Omega_K} \frac{d}{dr} \left(\frac{\Omega_K}{r} \right) - \alpha c_s^2 \left(2\zeta \frac{l_0}{r^2} + \zeta \eta \frac{\alpha c_s^2}{r v_r} \right) + \frac{q^-}{\rho} \quad (9)$$

$$B \equiv \left(1 - \zeta \eta \alpha^2 \frac{c_s^2}{v_r^2} \right) c_s \left[(\Omega_K^2 - \Omega^2)r + \frac{rc_s^2}{\Omega_K} \frac{d}{dr} \left(\frac{\Omega_K}{r} \right) \right] + (v_r^2 - c_s^2) \left[\frac{rc_s}{\Omega_K} \frac{d}{dr} \left(\frac{\Omega_K}{r} \right) \right] + \alpha \frac{c_s}{v_r} \left(2\zeta \frac{l_0}{r^2} + \zeta \eta \frac{\alpha c_s^2}{r v_r} \right) - \frac{q^-}{\rho v_r c_s} \quad (10)$$

$$D \equiv \left(\frac{\gamma + 1}{\gamma - 1} + 2\zeta \eta \alpha^2 \frac{c_s^2}{v_r^2} \right) v_r^2 - \left(\frac{2\gamma}{\gamma - 1} + \zeta \eta \alpha^2 \frac{c_s^2}{v_r^2} \right) c_s^2. \quad (11)$$

The zero of the denominator, $D = 0$, yields the well-known critical (or sonic) point condition $(v_r/c_s)^2 = 2\gamma/(\gamma - 1)$ (see, e.g., Narayan et al. 1997), modified by viscosity. The exact value of the Mach number $\mathcal{M}_{\text{cr}} \equiv |v_r/c_s|_{r_{\text{cr}}}$ at the critical point r_{cr} is given by the root of the equation

$$(\gamma + 1)\mathcal{M}_{\text{cr}}^4 - [2\gamma + 2\alpha^2(\gamma - 1)]\mathcal{M}_{\text{cr}}^2 + \alpha^2(\gamma - 1) = 0 \quad (12)$$

for our specific choice of viscosity description. For $\alpha \ll 1$, $\mathcal{M}_{\text{cr}}^2 \approx 2\gamma(\gamma + 1)^{-1}[1 + \alpha^2(\gamma - 1)(8\gamma - 1)(4\gamma^2)^{-1}]$.

2.2. Boundary Conditions and Method of Calculation

For spherical accretion, the widely used Bondi accretion rate is solely determined by the density and the temperature of accreting gas at infinity. To be more precise, however, there is no unique solution for a given density and temperature at infinity: the same boundary condition does allow subsonic (type I), transonic (type II), and unphysical (type III) solutions with different mass accretion rates (Bondi 1952). The additional requirement that the flow be transonic, i.e., regular at the critical point, becomes an additional constraint, which uniquely determines the solution and its accretion rate (cf. Parker 1963).

In rotating accretion flow, we expect one more physical quantity to be important: the angular momentum of the gas. In the slim disk formalism, the integration constant l_0 is an eigenvalue, and only a specific value of l_0 for given M , \dot{M} , α , ρ_{out} , and T_{out} admits a regular transonic solution (Muchotrzeb & Paczyński 1982; Abramowicz et al. 1988).

Spherical Bondi accretion has a critical point, which prevents the direct integration of the equations from the outer subsonic region to the inner supersonic region. This difficulty has been handled in two ways: either one starts with an arbitrarily chosen critical radius, integrates both inward and outward with the help of regularity conditions, and adjusts the critical radius until the outer and inner (if any) boundary conditions are satisfied (Bisnovatyi-Kogan & Blinnikov 1980; Quataert & Narayan 2000), or one starts with known outer boundary conditions such as density and temperature of gas plus initial choice of radial velocity (or equally mass accretion rate), integrates inward toward the critical point, checks if the velocity suddenly changes sign or diverges, adjusts the velocity (or the mass accretion rate) accordingly until the integrated radial velocity behaves normally even very close to the critical radius, extrapolates across the critical point when the adjustment is precise enough, and then integrates from there inward (Park 1990). This latter iteration procedure has some resemblance to the physical behaviors of the accretion flows. If the gas at the outer boundary starts to accrete with too small velocity (or mass accretion rate) than that of the transonic solution, the gas flow stays subsonic all the way, never passing the critical point (type I). On the other hand, if the gas starts to accrete with too large velocity, the velocity of the flow diverges before the critical point and becomes unphysical (type III). Only when the gas starts to accrete with the just right velocity, or equally mass accretion rate, can the flow pass through the critical point and become steady transonic flow (type II).

The dynamics of rotating accretion flows are similar except that we must include the added complications due to angular momentum and viscosity. The flow must have the right mass accretion rate and angular momentum for given density and temperature of gas at the outer boundary to pass through the critical point. To find such regular transonic solution, the angular momentum eigenvalue l_0 is searched by iteratively integrating the equations, either from the outer boundary (e.g., Muchotrzeb & Paczyński 1982; Abramowicz et al. 1988; Nakamura et al. 1997) or from the critical point in and out (Chakrabarti 1996; Narayan et al. 1997). Similar procedures are also required to find the subsonic accretion solutions or supersonic solutions with standing shocks onto compact objects with hard surfaces, such as white dwarfs or neutron stars, that satisfy specific outer and inner boundary conditions (Popham & Narayan 1991; Narayan & Medvedev 2003).

Since we are more interested in the mass accretion rate of the transonic flow for given boundary conditions at large radius,

we integrate from the outer boundary inward with the procedure used for spherical accretion as explained above (Park 1990). The basic parameters, the viscosity parameter α , and the adiabatic index γ are chosen first. In this work, we assume $\gamma = 5/3$ and $\alpha = 0.01$ unless noted otherwise. We then fix the density ρ_{out} and the temperature T_{out} of the gas at the outer boundary r_{out} . We also choose an integration constant l_0 . We start to integrate inward by arbitrarily choosing an initial guess for the mass accretion rate \dot{M} , which, along with other conditions, determines the radial velocity v_r from Equation (2) and then the angular velocity Ω at the outer boundary from Equation (4) to enable the initial integration. The initial guess for \dot{M} produces either a subsonic solution or an unphysical, diverging solution, and integration stops. We then adjust \dot{M} until the integration can proceed as close to the critical point as possible with a regular velocity profile. The bifurcation between subsonic and diverging solution is quite sharp, and the iterations can determine \dot{M} up to an arbitrary precision. Once the integration reaches close enough to the critical point, the flow solutions are extrapolated across the critical point to the supersonic region by an appropriate rational function, and the integration ensues from therein. The interpolation introduces minimal error because the supersonic part of non-transonic flow converges to the transonic flow at smaller radii (see, e.g., Bondi 1952; and Das 2007).

Since fixing l_0 and adjusting \dot{M} are equivalent to fixing \dot{M} and adjusting l_0 , and the transonic solutions exist only for a rather limited range of l_0 , we fix \dot{M} and adjust l_0 in most cases. Moreover, Equation (4) relates l_0 to the angular momentum at the outer boundary, l_{out} , and, therefore, adjusting l_0 is also equivalent to adjusting $l_{\text{out}} \equiv \Omega(r_{\text{out}})r_{\text{out}}^2$. Since the reference angular momentum against which l_{out} needs to be compared is $l_B \equiv r_B c_s(r_B) = GM/c_{s,\text{out}}$ which in fact is the Keplerian angular momentum at r_B if $r_B \gg r_{\text{Sch}}$, we define a dimensionless angular momentum measure $\lambda = l_{\text{out}}/l_B$. To summarize, we construct a global transonic solution for given ρ_{out} , T_{out} , and λ .

Since our integration starts from a finite radius rather than from infinity, we redefine the Bondi rate as $\dot{M}_B \equiv 4\pi\Lambda\gamma^{-3/2}(GM)^2\rho_{\text{out}}c_{s,\text{out}}^{-3}$. With our choice of a cooling function, the whole problem can be put into a dimensionless form, and the result, such as the dimensionless mass accretion rate $\dot{m} \equiv \dot{M}/\dot{M}_B$, is independent of the black hole mass M if the density is scaled in units of

$$\rho_0 \equiv \frac{m_p}{\sigma_T r_{\text{Sch}}} \simeq 1.7 \times 10^{-5} \left(\frac{M}{M_\odot}\right)^{-1} \text{ g cm}^{-3}, \quad (13)$$

where σ_T is the Thomson scattering cross section.

3. RESULT AND DISCUSSION

3.1. Flow Properties

Figure 1 shows typical solutions with different amount of angular momentum: high angular momentum (solid lines), intermediate angular momentum (dotted lines), and low angular momentum (dashed lines). By high angular momentum, we mean $\lambda \sim 1$, by low angular momentum, $\lambda \ll 1$, and by the intermediate angular momentum, between the two limits. The density and the temperature of gas at the outer boundary are the same for the three solutions: $T_{\text{out}} = 2.75 \times 10^9$ K and $\rho_{\text{out}} = 1.5 \times 10^{-6} \rho_0$ at $r_{\text{out}} = 10^3 r_{\text{Sch}}$. The dimensionless angular momenta of gas at the boundary and the mass accretion rate are $\lambda = 1.7$ and $\dot{m} = 0.05$

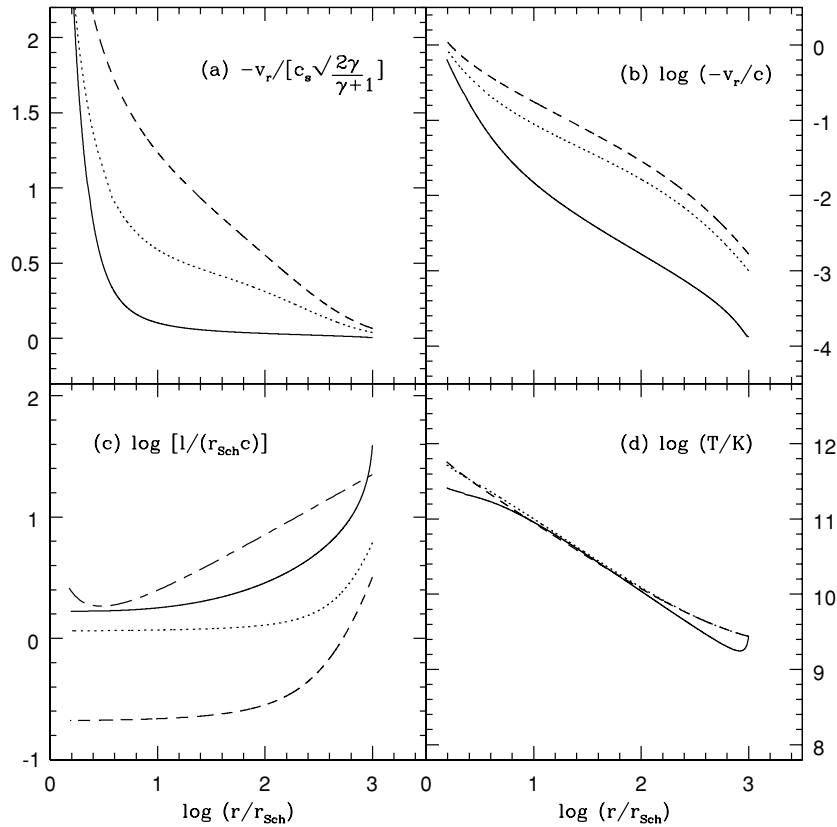


Figure 1. (a) Mach number, (b) velocity, (c) angular momentum, and (d) temperature profiles of typical high (solid lines), intermediate (dotted lines), and low angular momentum (dashed lines) solutions. The long–short dashed line in (c) is the Keplerian angular momentum for Paczyński–Wiita potential. See the text for details.

for high angular momentum flow, $\lambda = 0.27$ and $\dot{m} = 0.386$ for intermediate angular momentum flow, and $\lambda = 0.14$ and $\dot{m} = 0.643$ for low angular momentum flow. Most of the thermal energy is advected with the flow rather than radiated away, and temperature stays close to the virial value.

The flow with high angular momentum becomes supersonic at small radius $r_{\text{cr}} = 2.2r_{\text{Sch}}$ (solid line in Figure 1(a)) and the angular momentum (solid line in Figure 1(c)) is close to or a few times lower than the Keplerian value (short–long dashed line in Figure 1(c)). The radial velocity is significant but still smaller than the near free-fall velocity of spherical Bondi flow. This is a typical hot, radiatively inefficient advection-dominated accretion flow (ADAF) that has been extensively studied (e.g., Narayan & Yi 1994, 1995; Abramowicz et al. 1995; Narayan et al. 1997; Chen et al. 1997).

In spherical accretion, the flow passes the critical point at a much larger radius $r_{\text{cr}} \sim r_B$, and the flow becomes supersonic inside $\sim r_B$. But in rotating viscous accretion flow, a large part of the flow is subsonic well inside r_B because the rotation of the flow balances out gravity, and the value of r_{cr} depends on the angular momentum of the flow. A low angular momentum flow (dashed line in Figure 1(a)) has a critical point at a much larger radius $r_{\text{cr}} = 17r_{\text{Sch}}$ compared to the high angular momentum one. It has a larger radial infall velocity at the outer boundary as well because of smaller centrifugal force (Figure 1(b)), and the mass accretion rate is higher than that of the high angular momentum flow. These characteristics show that this low angular momentum flow has more resemblance to the spherical flow than to the disk flow as is expected. This type of flow solution is first discovered by Yuan (1999) and its dynamical and thermal properties have been comprehensively studied by Lu et al. (1999) and Yuan et al. (2000).

The flow with intermediate angular momentum (dotted lines) has a critical point at $r_{\text{cr}} = 3.2r_{\text{Sch}}$, and shows intermediate characteristics between the high and low angular momentum flow. The flow properties change from disklike to quasispherical as the angular momentum of the flow decreases. This is similar to the case of inviscid rotating accretion flow, which becomes disklike or quasispherical, depending on the angular momentum (Abramowicz & Zurek 1981). This transition of accretion flow from disklike to quasispherical in terms of critical radius position is described in detail by Yuan et al. (2000).

3.2. Mass Accretion Rate

In spherical accretion, the outer boundary is naturally selected to be outside the critical point, where the density and the temperature of gas stay roughly constant. In rotating viscous flow, the outer boundary is not naturally associated with the critical point which is at much smaller radius. So we consider two choices for the outer boundary radius: one at the Bondi radius, $r_B(T_{\text{out}})$, for given T_{out} and the other at a fixed radius regardless of T_{out} . The former choice is equivalent to setting the outer boundary at a virial temperature if we define the virial temperature as $T_{\text{vir}}(r) \equiv GMm_p/(2kr)$.

While original Bondi solutions are expressed in terms of the density and temperature of gas at infinity, our solutions start at a finite radius. But since the density and temperature of gas vary little from infinity to the Bondi radius in the Bondi solutions, we compare our solutions for the given density and temperature of gas at finite r_{out} against the Bondi solutions with the same density and temperature at infinity.

We first discuss the case where the outer boundary is set to be the Bondi radius, $r_{\text{out}} = GM/c_{s,\text{out}}^2 \propto T_{\text{out}}^{-1}$ for given T_{out} ,

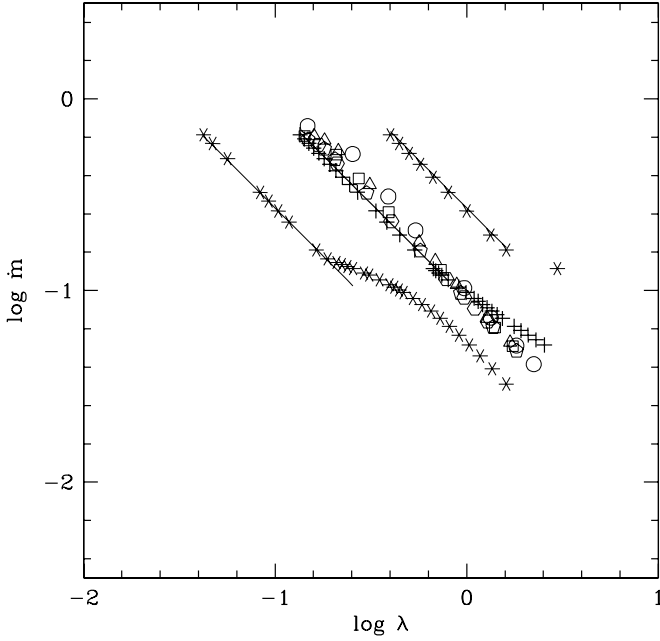


Figure 2. Mass accretion rate in units of the Bondi rate as a function of the angular momentum at the outer boundary in units of l_B for an outer boundary at the Bondi radius when the temperature at the outer boundary is equal to the virial temperature. Different symbols represent different temperature at the outer boundary: circles for $T_{\text{out}} = 1.1 \times 10^{10}$ K, triangles for $T_{\text{out}} = 5.5 \times 10^9$ K, squares for $T_{\text{out}} = 2.8 \times 10^9$ K, pentagons for $T_{\text{out}} = 1.2 \times 10^9$ K, hexagons for $T_{\text{out}} = 5.5 \times 10^8$ K, and crosses for $T_{\text{out}} = 1.1 \times 10^7$ K, but all for $\alpha = 0.01$. A series of star symbols on the left represent $T_{\text{out}} = 1.1 \times 10^7$ K and $\alpha = 0.003$ and those on the right $T_{\text{out}} = 1.1 \times 10^7$ K and $\alpha = 0.03$, respectively.

so that the solutions can be meaningfully compared with the Bondi solutions. The density at the outer boundary is either $\rho_{\text{out}} = 1.5 \times 10^{-6} \rho_0$ or $1.5 \times 10^{-9} \rho_0$. Since the whole set of equations can be rescaled in density except the cooling function q^- , the mass accretion rate then is simply proportional to ρ_{out} when cooling is not important. In such a case, the flow profile depends only on \dot{m} and not on the specific value of ρ_{out} . However, as the mass accretion rate \dot{M} approaches 0.1 times the Eddington mass accretion rate, $\dot{M}_{\text{Edd}} \equiv L_{\text{Edd}}/c^2$, cooling becomes important as in spherical accretion (Park 1990). In such a high $\dot{M}/\dot{M}_{\text{Edd}}$ case, the existence and the properties of the flow depend on the specific value of ρ_{out}/ρ_0 .

Figure 2 shows the mass accretion rate of constructed solutions as a function of the angular momentum at the outer boundary, in the \dot{m} versus λ plane. Symbols represent the solutions for different T_{out} : circles for $T_{\text{out}} = 1.1 \times 10^{10}$ K ($r_{\text{out}} = 2.5 \times 10^2 r_{\text{Sch}}$), triangles for $T_{\text{out}} = 5.5 \times 10^9$ K ($r_{\text{out}} = 5.0 \times 10^2 r_{\text{Sch}}$), squares for $T_{\text{out}} = 2.8 \times 10^9$ K ($r_{\text{out}} = 1.0 \times 10^3 r_{\text{Sch}}$), pentagons for $T_{\text{out}} = 1.1 \times 10^9$ K ($r_{\text{out}} = 2.5 \times 10^3 r_{\text{Sch}}$), and hexagons for $T_{\text{out}} = 5.5 \times 10^8$ K ($r_{\text{out}} = 5.0 \times 10^3 r_{\text{Sch}}$). All these solutions are calculated for $\rho_{\text{out}} = 1.5 \times 10^{-6} \rho_0$. The solutions for $T_{\text{out}} = 1.1 \times 10^7$ K ($r_{\text{out}} = 2.5 \times 10^5 r_{\text{Sch}}$), temperature suitable for the interstellar medium (ISM) in a galactic nucleus, have much larger r_{out} , and the bifurcation between subsonic to unphysical branch becomes even sharper. Since the critical mass accretion rate above which the hot, optically thin accretion disk does not exist also decreases as r_{out} increases (Abramowicz et al. 1995) and the Bondi rate increases as T_{out} decreases, we choose $\rho_{\text{out}} = 1.5 \times 10^{-9} \rho_0$ so that $\dot{M}/\dot{M}_{\text{Edd}}$ is in a range where solutions can be found. The mass accretion rates of these solutions are shown as crosses in the center of Figure 2.

We find that regardless of T_{out} , the mass accretion rate \dot{m} decreases as the angular momentum λ increases. It approaches the Bondi accretion rate as λ decreases. This change of mass accretion rate on the angular momentum is expected because given density and temperature at r_{out} , ρ , and H are fixed in the continuity equation (Equation (2)), and the mass accretion rate is determined solely by the radial velocity v_r . From Equation (3), the radial velocity is determined by the difference between the gravity and the centrifugal acceleration which is proportional to l^2/r^3 (at $r \gg r_{\text{Sch}}$). Larger angular momentum causes smaller infall velocity, and the mass accretion rate decreases and vice versa.

The mass accretion rate for the lowest angular momentum flow is quite close to the Bondi rate ($\dot{m} \sim 1$) while that for the highest angular momentum flow is roughly 20 times smaller than the corresponding Bondi rate ($\dot{m} \sim 0.05$). We also find that \dot{m} as a function of λ is rather insensitive to T_{out} , or equally r_{out} for $\dot{m} \gtrsim 0.1$: the slope of $\dot{m}(\lambda)$ has a tendency to become slightly flatter (from circles to crosses) as T_{out} decreases but the difference is not large.

Since we expect the flow profile, especially the radial velocity, to depend on the specific value of α , we also calculate the solutions for different values of α . The mass accretion rates of $\alpha = 0.003$ are shown as a series of stars in the left side of Figure 2 and that of $\alpha = 0.03$ are shown in the right side of Figure 2. Compared to the solutions for $\alpha = 0.01$ in the center denoted by crosses, lower α flows have smaller mass accretion rate and higher α flows have larger mass accretion rate. Larger α means stronger viscosity for given density and temperature, which causes larger radial velocity, and hence larger mass accretion rate, and vice versa for smaller α . The relation between \dot{m} and λ for $0.1 \lesssim \dot{m} \lesssim 1$ can be approximated by

$$\dot{m}(\lambda) = 0.09 \left(\frac{\alpha}{0.01} \right) \lambda^{-1}. \quad (14)$$

The three straight lines (from left to right) in Figure 2 show this fitting function for $\alpha = 0.003$, 0.01, and 0.03, respectively.

The mass accretion rate of the self-similar ADAF that has density ρ_{out} at r_{out} has the same dependence on ρ_{out} and r_{out} as the Bondi rate \dot{M}_B (Narayan & Yi 1994). Hence, the dimensionless mass accretion rate of self-similar ADAF is simply $\dot{m}_{\text{ADAF}} = 3.3\alpha$. Since ADAF generally refers to $\lambda \sim 1$ flow and $\dot{m}(\lambda = 1) \simeq 3\dot{m}_{\text{ADAF}}$, we find that our solutions have approximately three times higher mass accretion rates than those of self-similar ADAFs. The difference is probably due to the fact that the density and velocity of global ADAFs do not exactly follow the self-similar form, especially near the outer boundary (Narayan et al. 1997; Chen et al. 1997).

For given T_{out} , the lower limit on the mass accretion rate is determined by the Keplerian angular momentum barrier. A smaller mass accretion rate demands smaller radial infall velocity. From Equation (4), smaller $|v_r|$ requires larger Ω , and eventually Ω becomes larger than the Keplerian value Ω_K at r_{out} for too small mass accretion rate. Gas cannot accrete in steady state when the angular momentum is much larger than the Keplerian one, and therefore no solution exists when $\lambda \gtrsim 3$. Although we could determine \dot{m} below $\dot{m} \simeq 0.1$ from shooting until λ approaches ~ 1.5 – 3 , in many cases we failed to construct the full transonic solutions down to the inner boundary. The difficulty is much more severe for small α : the bifurcation between subsonic and unphysical occurs at a large radius and computing accuracy is not enough to integrate all the way down to the horizon. So we have limited confidence in the solutions

below $\dot{m} \lesssim 0.2$ for $\alpha = 0.003$ and 0.03 . The upper limit on the mass accretion rate on the other hand is determined by the Bondi accretion rate itself. The lowest angular momentum flow has its mass accretion rate already quite close to the Bondi rate, which is the mass accretion rate for zero angular momentum flow. Thus any higher mass accretion flow will end up on the unphysical branch of solutions in spherical Bondi flow (type III), with minimum effect due to the angular momentum.

We can think of extending the velocity versus radius diagram of Bondi (1952) to a similar one with the angular momentum effect added. What angular momentum does is to lower the critical mass accretion rate for the transonic flow. As the angular momentum of the flow increases, the critical mass accretion rate decreases, and the rotating accretion flow accretes transonically at a critical mass accretion rate lower than the original Bondi accretion rate. On the other hand, if the angular momentum of the flow decreases, the critical mass accretion rate increases up to the Bondi accretion rate which is the critical mass accretion rate for zero angular momentum flow, above which no transonic steady-state rotating accretion flow exists. Since Equation (14) gives $\dot{m} > 1$ for $\lambda < 9\alpha$ and \dot{m} cannot be greater than unity, it looks like there is no solution for $\lambda < 9\alpha$. However, we are using the slim disk formulation with a simple viscosity prescription to describe what is really a two-dimensional quasispherical flow, especially for lowest angular momentum flow; so the non-existence of solutions below the lower limit on λ is probably caused by the approximate physical descriptions of the flow, especially the overestimated viscosity for the low or no angular momentum flow. Surely, we will have a spherical Bondi flow when the angular momentum is zero. Therefore, we expect that steady flow probably exists even below $\lambda \sim 9\alpha$ and

$$\dot{m} \simeq 1 \quad \text{for } \lambda \lesssim 9\alpha. \quad (15)$$

We conclude that the steady-state, transonic hot accretion flow exists only when the mass accretion rate is within a certain range or the angular momentum at the outer boundary is below a certain maximum value. For our specific choice of parameters and conditions, the range in the mass accretion rate is

$$\dot{m}_{\text{cr}} \lesssim \dot{m} \leq 1, \quad (16)$$

where $\dot{m}_{\text{cr}} = \dot{m}(\lambda_{\text{cr}})$ is the mass accretion rate of the flow with maximum possible angular momentum at the outer boundary. Our calculations suggest $\lambda_{\text{cr}} \lesssim 3$ and $\dot{m}_{\text{cr}} \sim 0.05$ for $\alpha = 0.01$.

Now we discuss flows with the outer boundary temperature different from the virial temperature. For example, when the cool, outer geometrically thin disk is attached to the hot inner accretion disk, the temperature at the outer boundary will be much lower than the virial temperature (Narayan et al. 1997). So we fix $r_{\text{out}} = 10^3 r_{\text{Sch}}$ but vary T_{out} . The outer boundary density is the same at $\rho_{\text{out}} = 1.5 \times 10^{-6} \rho_0$. Figure 3 shows the mass accretion rate again in the \dot{m} versus λ plane. Symbols are the same as in Figure 2, except circles for $T_{\text{out}} = 3.6 \times 10^9$ K, triangles for $T_{\text{out}} = 2.2 \times 10^9$ K, squares for $T_{\text{out}} = 1.1 \times 10^9$ K, pentagons for $T_{\text{out}} = 5.5 \times 10^8$ K, and hexagons for $T_{\text{out}} = 2.0 \times 10^8$ K.

Again, solutions exist only in a limited range of \dot{m} , or equally λ . But this time both upper and lower limits on \dot{m} vary with T_{out} . The reason for the difference is that r_{out} is fixed and not related to T_{out} whereas it is related to T_{out} in Bondi solutions. As in the previous choice of the boundary, the lower limit on \dot{m} is from the Keplerian angular momentum barrier. However, the upper limit is determined for a different reason in this case. As

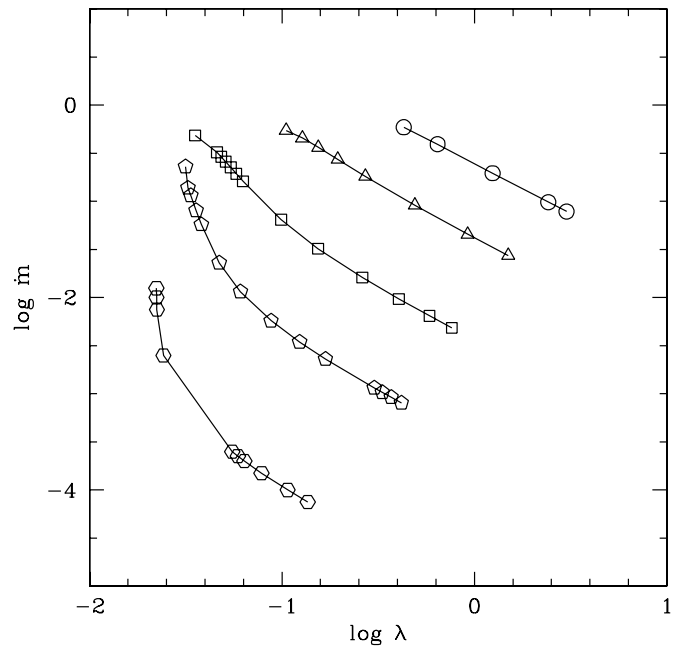


Figure 3. Mass accretion rate in units of the Bondi rate as a function of the angular momentum at the outer boundary in units of l_B for a fixed outer boundary at $r_{\text{out}} = 10^3 r_{\text{Sch}}$ and $\alpha = 0.01$. Symbols represent the same as in Figure 2, except circles for $T_{\text{out}} = 3.6 \times 10^9$ K, triangles for $T_{\text{out}} = 2.2 \times 10^9$ K, squares for $T_{\text{out}} = 1.1 \times 10^9$ K, pentagons for $T_{\text{out}} = 5.5 \times 10^8$ K, and hexagons for $T_{\text{out}} = 2.0 \times 10^8$ K.

the mass accretion rate for given boundary conditions increases, the radial infall velocity at the outer boundary should increase. But the increasing radial infall velocity eventually becomes larger than the sound speed at the boundary. The whole flow becomes supersonic from the outer boundary to the innermost radius. Since we are looking for transonic solutions that uniquely determine the mass accretion rate, we disregard these supersonic branch of solutions, and no transonic solutions exist above certain upper limit on \dot{m} . This upper limit on \dot{m} decreases as T_{out} decreases because the sound speed decreases with T_{out} and the flow becomes supersonic at smaller radial velocity, or mass accretion rate, causing rapid decrease of the upper limit on \dot{m} with decreasing T_{out} .

The dependence of \dot{m} on λ is also different. Again, \dot{m} decreases as λ increases, but is not inversely proportional to λ , nor is independent of T_{out} . Cooler flow, i.e., lower T_{out} , has lower mass accretion rate \dot{m} for a given λ . When $\lambda = 0.1$, \dot{m} for $T_{\text{out}} = 2.2 \times 10^9$ K is ~ 1 while that for $T_{\text{out}} = 2.0 \times 10^8$ K is as low as $\sim 10^{-4}$. This means that if gas is injected into a given radius with near-Keplerian angular momentum but with temperature much below the virial temperature at that radius, the mass accretion rate can be a few orders of magnitude below the Bondi accretion rate.

4. SUMMARY

We have constructed global solutions of the rotating, viscous accretion flow within the framework of a height-averaged, slim α disk with varying amount of specific angular momentum λ at the outer boundary. We find that the low angular momentum flow, the flow with $\lambda \ll 1$, resembles the spherical Bondi flow, and its mass accretion rate approaches the Bondi accretion rate for the same density and temperature at the outer boundary. The high angular momentum flow, the flow with $\lambda \sim 1$, on the other hand, is the conventional hot accretion disk with advection, but

its mass accretion rate can be significantly smaller than the Bondi accretion rate for the same density and temperature at the outer boundary.

We also find that solutions exist only within a limited range of the dimensionless mass accretion rate \dot{m} , the mass accretion rate in units of the Bondi accretion rate. When the temperature at the outer boundary is equal to the virial temperature at that radius, solutions exist only when $\dot{m}_{\text{cr}} \lesssim \dot{m} \leq 1$ because below \dot{m}_{cr} the angular momentum of the flow becomes higher than the Keplerian value, and the steady accretion is not possible. The exact value of \dot{m}_{cr} as a function of the viscosity parameter α is not known, but is ~ 0.05 for $\alpha = 0.01$. The upper limit on the mass accretion rate is the Bondi accretion rate since it is the mass accretion rate of zero angular momentum flow. Moreover, we also find that the dimensionless mass accretion rate is roughly independent of the radius of the outer boundary but inversely proportional to the angular momentum at the outer boundary in units of the Keplerian angular momentum at that same radius and proportional to the viscosity parameter, $\dot{m} \simeq 9.0 \alpha \lambda^{-1}$ when $0.1 \lesssim \dot{m} \lesssim 1$. When the temperature at the outer boundary is much less than the virial temperature, the mass accretion rate can be a few orders of magnitude smaller than the Bondi accretion rate.

The fact that the mass accretion rate can be smaller than the Bondi accretion rate and depends on the angular momentum of gas at the outer boundary could have interesting implications for many astrophysical accretion systems, especially underluminous active galactic nuclei and galactic centers.

Although we now have a better understanding of the behavior of rotating, viscous accretion flows with varying amount of angular momentum, the precise numerical values presented in this work are expected to contain some uncertainties because these hot accretion flows are certain to have real two-dimensional structures, and the one-dimensional, height-averaged approximation adopted in this work will only approximately describe the real flow. Hence, more precise analyses of these accretion flow including other relevant physics such as shocks (Chakrabarti & Das 2004), outflows (Stone et al. 1999), or radiative heating (Park & Ostriker 1999, 2001, 2007; Yuan et al. 2009; Proga et al. 2008) will require careful multi-dimensional studies (see, e.g., Proga 2007; Kurosawa & Proga 2008; and Proga et al. 2008 for current multi-dimensional studies).

We thank Jerry Ostriker for many insightful discussions and careful reading of the manuscript. We also thank the referee, Ramesh Narayan, for useful comments which significantly improved this paper. This work was supported by the Korea Research Foundation Grant funded by the Korean Government (MOEHRD; KRF-2007-013C00028) and also by the National Research Foundation of Korea (NRF) grant funded by the Korea government (MEST; No. 2009-0062868).

REFERENCES

- Abramowicz, M., Chen, X., Kato, S., Lasota, J.-P., & Regev, O. 1995, *ApJ*, **438**, L37
- Abramowicz, M. A., Czerny, B., Lasota, J. P., & Szuszkiewicz, E. 1988, *ApJ*, **332**, 646
- Abramowicz, M. A., & Zurek, W. H. 1981, *ApJ*, **246**, 314
- Bisnovatyi-Kogan, G. S., & Blinnikov, S. I. 1980, *MNRAS*, **191**, 711
- Bondi, H. 1952, *MNRAS*, **112**, 195
- Chakrabarti, S. K. 1996, *ApJ*, **464**, 664
- Chakrabarti, S. K., & Das, S. 2004, *MNRAS*, **349**, 649
- Chen, X., Abramowicz, M. A., & Lasota, J.-P. 1997, *ApJ*, **476**, 61
- Das, S. 2007, *MNRAS*, **376**, 1659
- Kurosawa, R., & Proga, D. 2008, *ApJ*, **674**, 97
- Lu, J.-F., Gu, W.-M., & Yuan, F. 1999, *ApJ*, **523**, 340
- Muchotrzeb, B., & Paczyński, B. 1982, *Acta Astron.*, **32**, 1
- Nakamura, K. E., Kusunose, M., Matsumoto, R., & Kato, S. 1997, *PASJ*, **49**, 503
- Narayan, R., Kato, S., & Honma, F. 1997, *ApJ*, **476**, 49
- Narayan, R., & Medvedev, M. V. 2003, *MNRAS*, **343**, 1007
- Narayan, R., & Yi, I. 1994, *ApJ*, **428**, L13
- Narayan, R., & Yi, I. 1995, *ApJ*, **452**, 710
- Paczynski, B., & Wiita, P. J. 1980, *A&A*, **88**, 23
- Park, M.-G. 1990, *ApJ*, **354**, 83
- Park, M.-G., & Ostriker, J. P. 1999, *ApJ*, **527**, 247
- Park, M.-G., & Ostriker, J. P. 2001, *ApJ*, **549**, 100
- Park, M.-G., & Ostriker, J. P. 2007, *ApJ*, **655**, 88
- Parker, E. N. 1963, *Interplanetary Dynamical Processes* (New York: Interscience)
- Popham, R., & Narayan, R. 1991, *ApJ*, **370**, 604
- Proga, D. 2007, *ApJ*, **661**, 693
- Proga, D., Ostriker, J. P., & Kurosawa, R. 2008, *ApJ*, **676**, 101
- Quataert, E., & Narayan, R. 2000, *ApJ*, **528**, 236
- Shakura, N. I., & Sunyaev, R. A. 1973, *A&A*, **24**, 337
- Stone, J. M., Pringle, J. E., & Begelman, M. C. 1999, *MNRAS*, **310**, 1002
- Svensson, R. 1982, *ApJ*, **258**, 335
- Yuan, F. 1999, *ApJ*, **521**, L55
- Yuan, F., Peng, Q., Lu, J.-f., & Wang, J. 2000, *ApJ*, **537**, 236
- Yuan, F., Xie, F., & Ostriker, J. P. 2009, *ApJ*, **691**, 98